Supporting Information

Semicarbonized Subwavelength-Nanopore-Structured Nanocellulose Paper for Application in Solar Thermal Heating

*Thanakorn Yeamsuksawat, Yoshitaka Morishita, Jun Shirahama, Yintong Huang, Takaaki Kasuga, Masaya Nogi, Hirotaka Koga**

SANKEN (The Institute of Scientific and Industrial Research), Osaka University, 8-1 Mihogaoka, Ibaraki, Osaka 567-0047, Japan

*Corresponding Author

Hirotaka Koga, E-mail: hkoga@eco.sanken.osaka-u.ac.jp

Supporting Figures

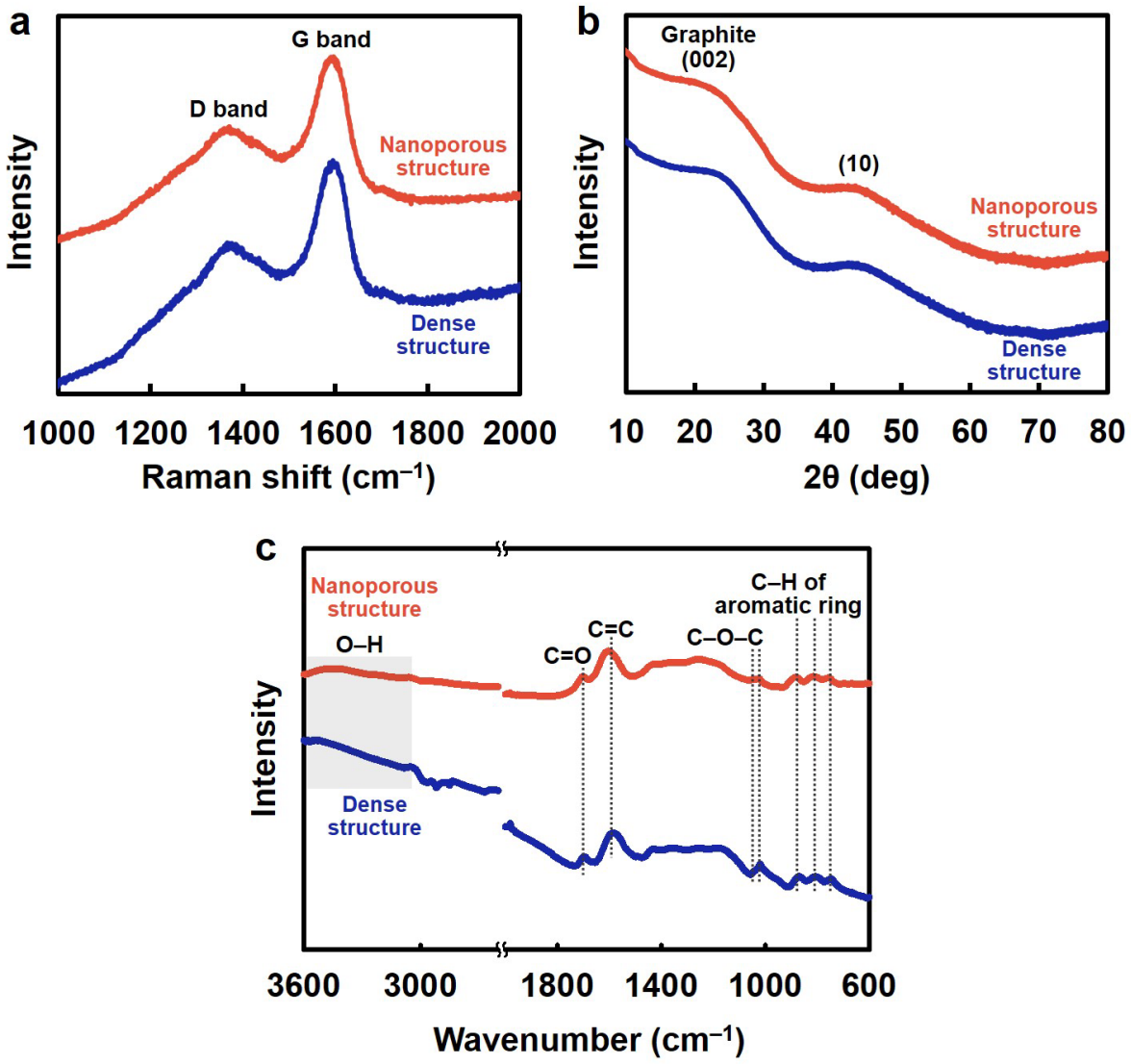

Figure S1. Molecular structures of carbonized nanopapers exhibiting nanoporous and dense structures. (a) Raman, (b) X-ray diffraction (XRD), and (c) Fourier-transform infrared (FT-IR) spectra of nanopaper carbonized at 500 °C exhibiting nanoporous or dense structures.

Regardless of the porous structure of the nanopaper, the Raman, XRD, and FT-IR spectra of both carbonized nanopapers were similar. In the Raman spectra, the G and the D bands were associated with the graphitic sp^2-hybridized carbon domains and the disordered graphitic carbon structures (e.g., edge of graphitic domains and in-plane imperfections)[1], respectively.

There was no large difference of the intensity ratio of D and G band peaks (I_D/I_G) between the carbonized nanopapers exhibiting nanoporous (I_D/I_G: 0.748) and dense structures (I_D/I_G: 0.766). In the XRD spectra, two broad peaks associated with the crystalline reflections (002) and the two-dimensional reflections (10) of graphite appeared at approximately 22° and 44°.[2] The graphite crystallite sizes in the stacking and in-plane directions (L_c and L_a, respectively) were estimated using these peaks and Scherrer's formula.[2] There was no large difference of the graphite crystallite sizes between the carbonized nanopapers exhibiting nanoporous (L_c: 0.87 nm, L_a: 1.84 nm) and dense structures (L_c: 0.85 nm, L_a: 1.83 nm). FT-IR spectra also suggested that the chemical structures of the carbonized nanopapers were similar. These results suggested that the nanopapers exhibited negligibly different molecular structures. This was possibly because the nanopapers had been carbonized at the same temperature.

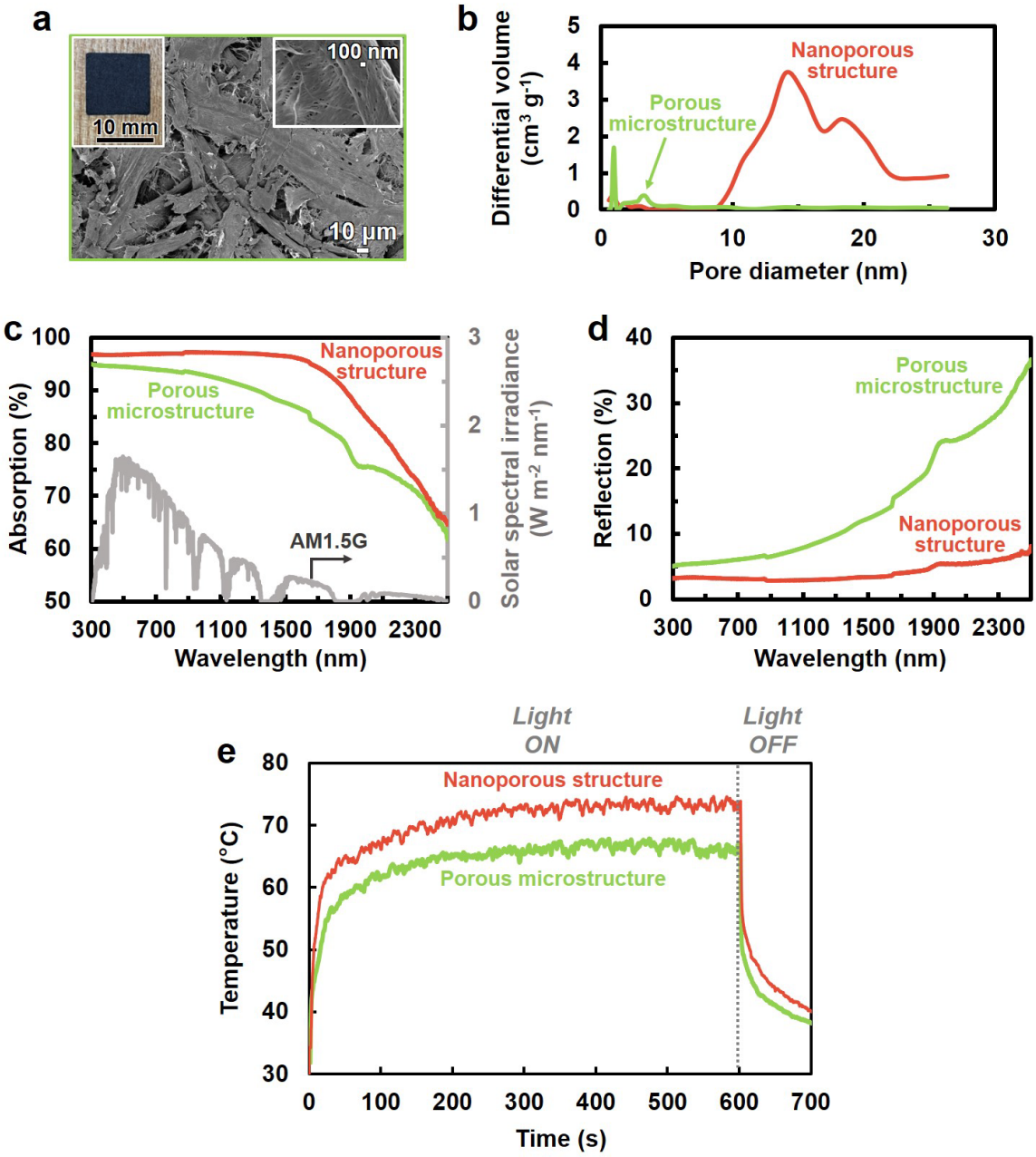

Figure S2. Porous structures, light absorption and reflection measurements, and solar thermal heating performances of cellulose pulp paper carbonized at 500 °C exhibiting porous microstructures. (a) Optical and field-emission scanning electron microscopy (FE-SEM) images of carbonized cellulose pulp paper exhibiting porous microstructures; (b) pore size distribution curves of carbonized cellulose pulp paper exhibiting porous microstructures and carbonized nanopaper exhibiting nanoporous structures, (c) solar spectral irradiance (AM1.5G) and UV–vis–NIR absorption, (d) reflection, and (e) solar thermal heating

performances of carbonized cellulose pulp paper exhibiting porous microstructures and carbonized nanopaper irradiated under 1 sun exhibiting nanoporous structures.

The cellulose pulp paper exhibiting porous microstructures was prepared using *tert*-butyl alcohol by hot pressing, and was treated with iodine and then carbonized at 500 °C. The carbonized cellulose pulp paper exhibited a few nanopores (size of the order of several nanometers) and pulp-fiber-network-derived microscale pores (**Figure S2a** and **b**). The carbonized cellulose pulp paper exhibiting porous microstructures showed lower light absorption and higher light reflection than the carbonized nanopaper exhibiting nanoporous structures (**Figure S2c** and **d**), indicating that the tailored carbonized nanopaper nanoporous structures had enhanced light absorption by suppressing light reflection. Owing to the enhanced light absorption, the carbonized nanopaper exhibiting nanoporous structures afforded higher solar thermal heating performance (approximately 73.9 ± 0.80 °C) than the carbonized cellulose pulp paper exhibiting porous microstructures (68.2 ± 0.96 °C) (**Figure S2e**).

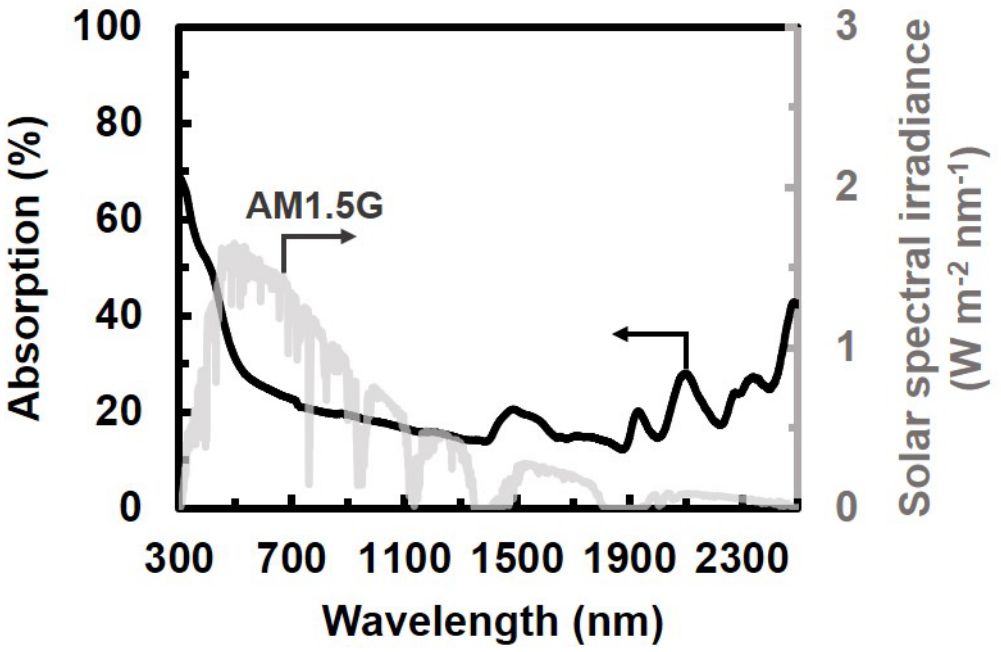

Figure S3. UV–vis–NIR absorption spectrum of original nanopaper and corresponding solar spectral irradiance (AM1.5G).

The original nanopaper exhibited poor light absorption and solar thermal heating (*i.e.*, the equilibrium temperature was only 37.9 °C for the nanopaper irradiated under 1 sun), indicating that the nanopaper must be carbonized for application to solar light absorption and thermal heating.

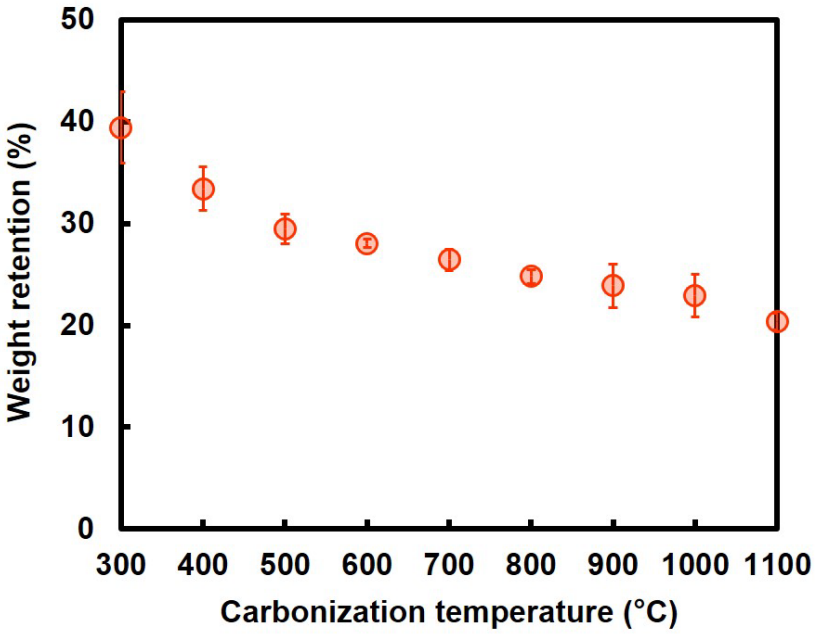

Figure S4. Weight retention of nanopaper exhibiting nanoporous structures carbonized at different temperatures.

The weight retention of the nanopaper exhibiting nanoporous structures was decreased from approximately 39.4 to 20.4% with increasing carbonization temperatures from 300 to 1100 °C, respectively.

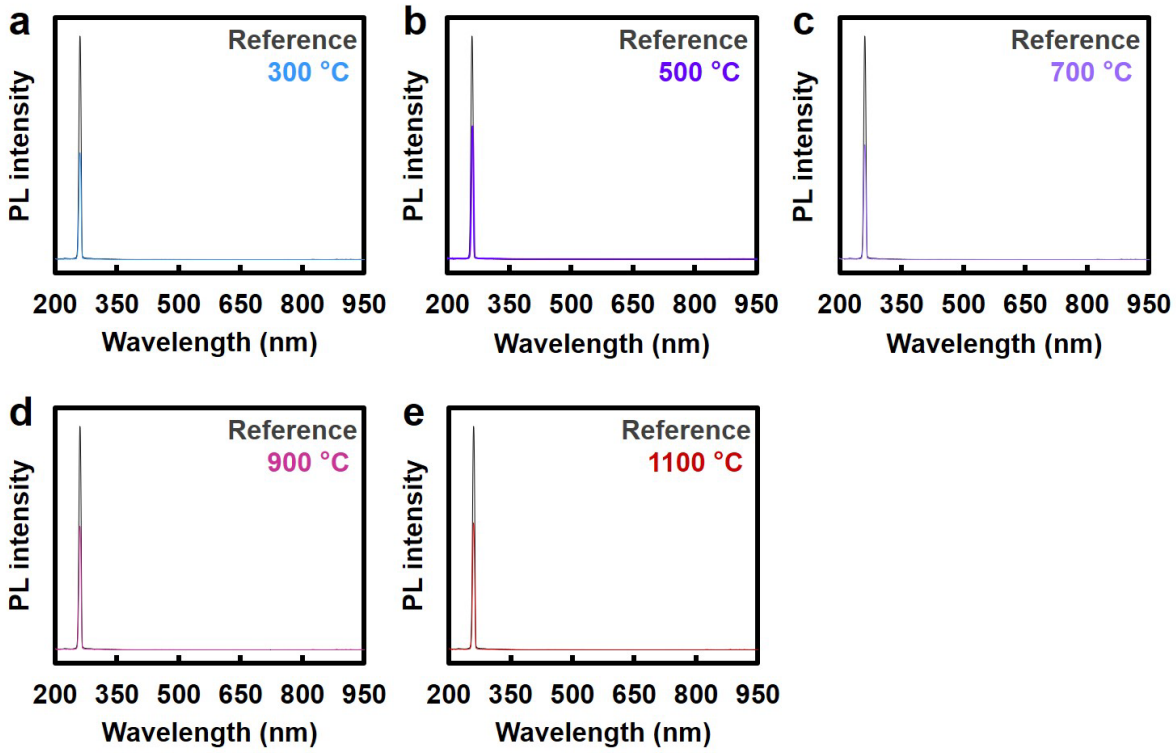

Figure S5. Photoluminescence (PL) spectra of nanopaper exhibiting nanoporous structures carbonized at (a) 300, (b) 500, (c) 700, (d) 900, and (e) 1100 °C.

Regardless of the carbonization temperature, the carbonized nanopapers exhibited almost no PL, indicating that most of the light absorbed by the carbonized nanopaper had been converted into heat.

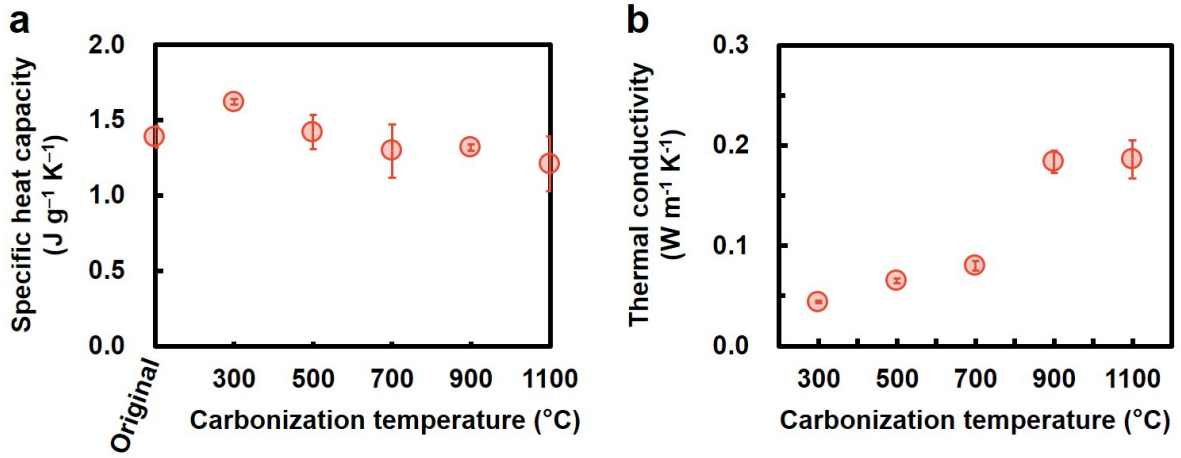

Figure S6. Thermal properties of carbonized nanopapers. (a) Specific heat capacity and (b) through-plane thermal conductivity of nanopaper exhibiting nanoporous structures carbonized at different temperatures.

Although the original nanopaper specific heat capacity was ~1.39 J g^{-1} K^{-1}, that of the nanopaper carbonized at 1100 °C was ~1.21 J g^{-1} K^{-1}, suggesting that the carbonized nanopaper specific heat capacity had negligibly changed (**Figure S6a**). The carbonized nanopaper through-plane thermal conductivity gradually increased from 0.04 to 0.19 W m^{-1} K^{-1} as the carbonization temperature was increased from 300 to 1100 °C, respectively (**Figure S6b**). Such gradual increase in through-plane thermal conductivity with increasing carbonization temperature would also cause the gradual decrease in the equilibrium surface temperature of the carbonized nanopaper under 1 sun irradiation (see also **Figure 4a**).

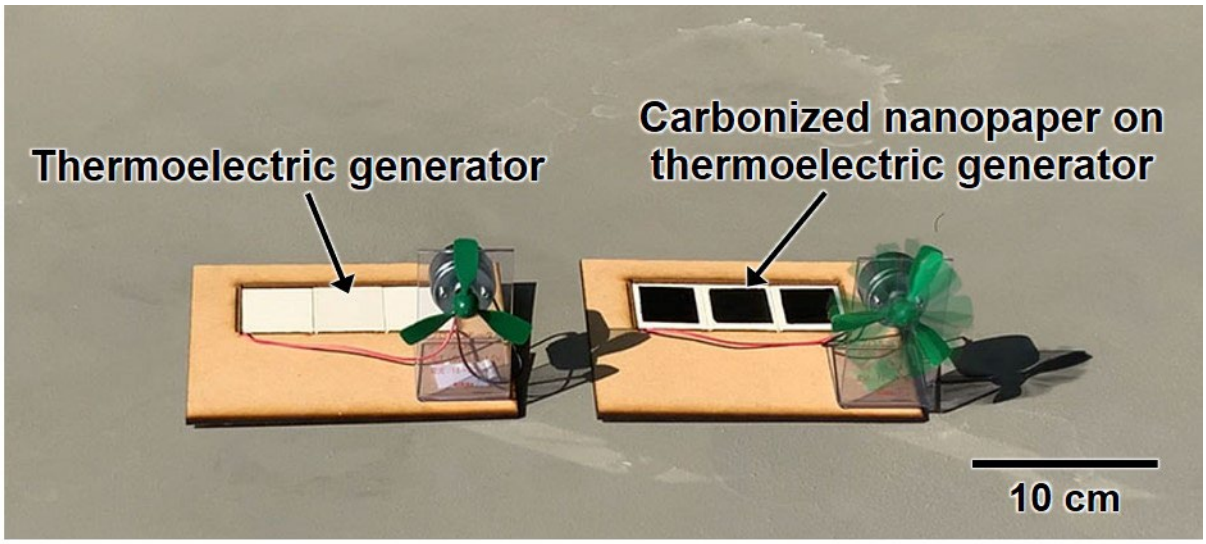

Figure S7. Solar-driven thermoelectric power generation using nanopaper carbonized at 500 °C.

To demonstrate the importance of solar thermal heating, the nanopaper carbonized at 500 °C was applied to thermoelectric power generation. As shown in **Figure S7**, three pieces (3.5 cm × 3.5 cm) of the nanopaper carbonized at 500 °C were adhered to a commercial thermoelectric power generator to fabricate a thermoelectric power generation module. On a sunny day, natural sunlight was irradiated on one side of the carbonized nanopaper, and this module generated enough electricity to run the propeller motor (working voltage: 0.4–1.5 V, working current: 16–20 mA). Thus, the nanopaper carbonized at 500 °C exhibited excellent solar thermal heating and was applied to solar-driven thermoelectric power generation.

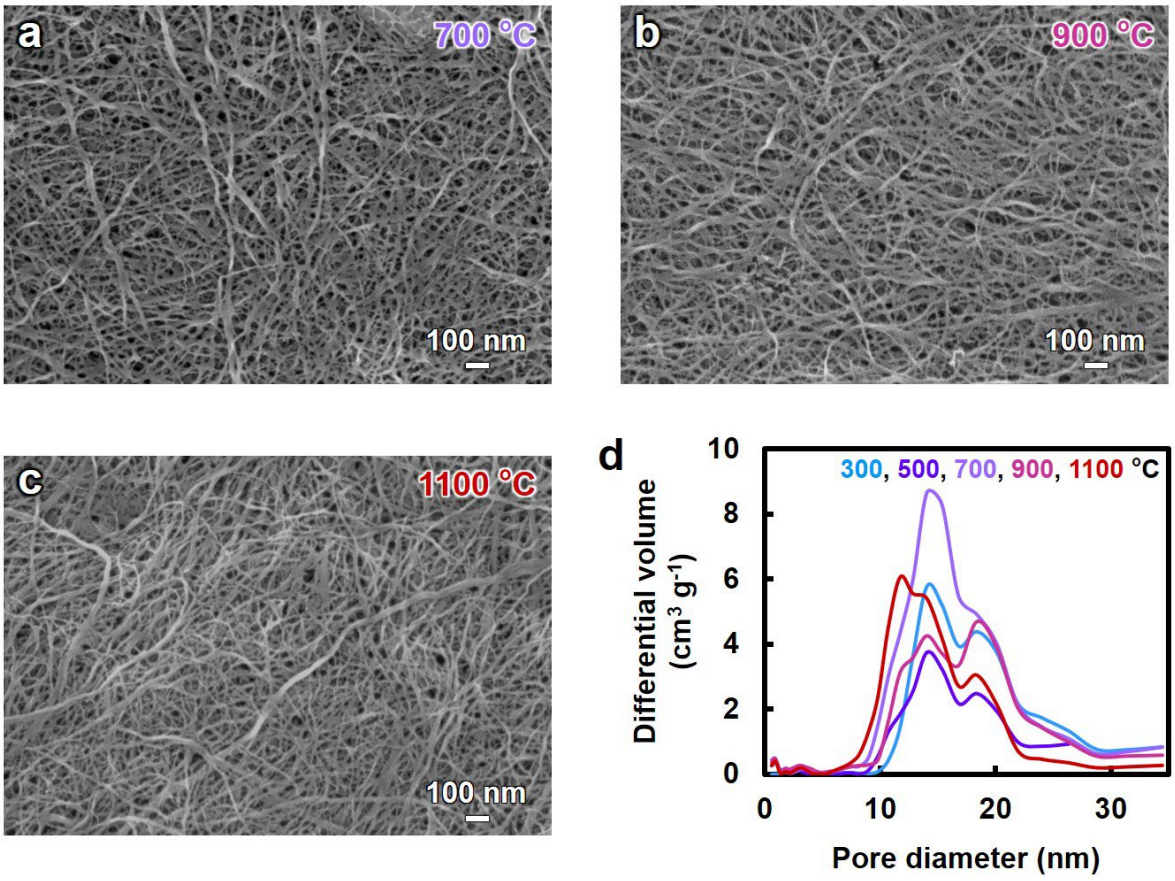

Figure S8. Nanoporous structures of nanopapers carbonized at different temperatures. FE-SEM images of nanopaper exhibiting nanoporous structures carbonized at (a) 700, (b) 900, or (c) 1100 °C. (d) Pore size distribution curves of nanopapers carbonized at different temperatures.

The FE-SEM images and pore size distribution curves suggested that the carbonized nanopapers exhibited negligibly different nanoporous structures regardless of the carbonization temperature.

References

(1) Dresselhaus, M. S.; Jorio, A.; Souza Filho, A. G.; Saito, R. Defect Characterization in Graphene and Carbon Nanotubes Using Raman Spectroscopy. *Philos. Trans. Royal Soc. A* **2010**, *368*, 5355–5377.

(2) Biscoe, J.; Warren, B. E. An X-Ray Study of Carbon Black. *J. Appl. Phys.* **1942**, *13*, 364–371.